Integrative Bioscience Nexus

Biologica Aid

Article

Corchorus olitorius and *Moringa oleifera* Manage Alpha-amylase and Alpha-glucosidase in Type 2 Diabetes: An *in vitro* and *in silico* Approach

Gobindo Kumar Paul[1]*, Tanvir Ahammad[2], Md. Abu Saleh[2]

[1] Bangladesh University of Professionals, Mirpur Cantonment Dhaka-1216, Bangladesh

[2] Microbiology Laboratory, Department of Genetic Engineering and Biotechnology, University of Rajshahi, Rajshahi-6205, Bangladesh

* Correspondence: gobindo.kumar@bup.edu.bd

Abstract: This work investigated the potential of *C. olitorius* and *M. oleifera* leaves and seeds as sources of bioactive compounds for T2DM treatment. We used *in silico* approaches to examine their inhibitory effects against alpha-amylase and alpha-glucosidase, two key enzymes in carbohydrate metabolism. Antioxidant activity tests revealed IC_{50} values of 108.96 µg/mL and 139.67 µg/mL for *C. olitorius* leaves and seeds, respectively, while *M. oleifera* leaves and seeds exhibited IC_{50} values of 132.15 µg/mL and 174.86 µg/mL, respectively. Cytotoxicity assays against *Artemia salina* indicated lower toxicity for leaf extracts compared to seed extracts. A comprehensive review of chromatography studies identified 223 phytochemicals from both plants. Among these, prunol, stigmasterol, and acarbose (control) showed the most favorable binding affinities to alpha-amylase, with binding free energies of -9.3, -9.4, and -7.9 Kcal/mol, respectively. For alpha-glucosidase, rutin, apigetrin, and acarbose (control) displayed binding energies of -8.9, -8.1, and -7.0 Kcal/mol, respectively. Molecular dynamics parameters (RMSD, SASA, Rg, RMSF, and H-bonds) demonstrated that stigmasterol and rutin exhibited the highest stability, suggesting their strong potential as competitive inhibitors. ADMET analysis further confirmed the favorable physicochemical, pharmacokinetic, and safety profiles of these compounds, positioning them as promising candidates for drug development. However, further *in vivo*, *in vitro*, and clinical studies are required to confirm their therapeutic efficacy in managing type 2 diabetes.

Keywords: Diabetes, Antioxidant, Cytotoxicity, Molecular docking, and ADMET

Academic Editor: Md. Arif Khan

Received: 10 April 2026
Revised: 15 May 2026
Accepted: 28 May 2026
Published: 05 July 2026

1. Introduction

Diabetes mellitus (DM) is a chronic metabolic illness in which the pancreas does not produce enough insulin or the body does not use it adequately, resulting in excessive blood glucose levels. Type 2 diabetes mellitus (T2DM) is a fast-growing global health concern. According to the International Diabetes Federation's 2023 projection, roughly 476 million people worldwide suffer with diabetes. Individuals with T2DM are at a higher risk of different problems and are more vulnerable to common infections, which can lead to serious illnesses such as renal damage, cognitive decline, and cancer. This metabolic condition is characterized by chronic hyperglycemia and insulin resistance. Hyperglycemia occurs when pancreatic cells fail to produce enough insulin, causing increased blood glucose levels.

Inhibiting the digestion of dietary carbohydrates, which reduces glucose absorption, is an important method for treating postprandial hyperglycemia in type 2 diabetes.

In the digestive tract carbohydrates are split into monosaccharides by the enzyme alpha-amylase first. These monosaccharides are subsequently transformed into glucose by alpha-glucosidase before being absorbed into the bloodstream. It can reduce blood sugar levels by slowing the digestion of carbohydrates by inhibiting the activities of alpha-amylase and alpha-glucosidase. The management of T2DM has been aided by the development of synthetic medications such as oral hypoglycemic treatments including metformin, sulfonylureas, thiazolidinediones, biguanides, meglitinides and dipeptidyl peptidase-IV inhibitors. However, long-term use of these medications often leads to adverse effects like liver dysfunction, hyperglycemia, and gastrointestinal issues. This highlights the urgent need for the development of novel inhibitors that are both effective and exhibit low toxicity. In this context, medicinal plants offer a promising alternative for drug discovery due to their lower toxicity, specificity, and wide availability.

Since ancient times, various plants have been widely used as treatments for diverse diseases which are one of the most effective medicinal compound sources and well-known for their potential therapeutic outcome [1], [2], [3], [4], [5]. From the crude extracts of alkaloids, flavonoids, terpenes, proteins and various glycosides several phytochemicals were isolated, purified, and identified [4]. Various plant bioactive components such as, flavonoids, polyphenols, saponins, alkaloids, terpenes, quinones, lignins, tannins, pro-anthocyanidins, steroids, thiosulfonates, polysaccharides and coumarins etc. are eminent bioactive phytochemicals that are noticed to have activities as an antiviral [6], [7], antifungal [8] and antibacterial [5], [9], [10], [11], [12]. Nowadays, near about 25% of the prescribed drugs are from the plant origin. Phytochemicals provide various approaches for the findings of antiviral agents with tremendous pharmacological effects. Yet people count on traditional plants and their compounds for their primary health care in numerous parts of the world. Besides, for the treatment of an uncountable inflictions and diseases, approximately 2500 medicinal plant species have been used worldwide [12], [13], [14], [15], [16], [17]. These natural compounds have been acknowledged to have antiviral activity and they can be used as a commencement point to search feasible bioactive candidates against tpye-2 diabetes [5], [18], [19].

Many plants having antioxidant potential provide the health benefits [20]. Free radicals cause oxidative stress in the body and are implicated in the processes of diabetes and neurodegenerative and inflammatory diseases [21], [22]. Antioxidants neutralize free radicals and reduce oxidative stress to avoid oxidation [23], [24]. Different plant species such as *Vinca rosea* (Nayantara), *Corchorus olitorius* (Jute) and *Moringa oleifera* (Moringa), *Allium sativum* (Garlic), *Trigonella foenum* (Fenugreek) and their bioactive compounds such as phenolics and flavonoids are found to have blood glucose lowering effects and potential therapeutic benefits.

The present work is aimed at evaluating the antioxidant and cytotoxic properties of *C. olitorius* and *M.oleifera* leaves and seeds under laboratory conditions. Then phytochemicals for both types were obtained from deep chromatography analysis and *in silico* analysis was used to find possible components of these extracts that can interact with the proteins of alpha-amylase and alpha-glucosidase of T2DM. The investigation indicated the potential therapeutic value of *C. olitorius* and *M. oleifera* leaves and seeds and their application as source of anti-diabetic and antioxidant chemicals. The *in silico* technique adds computational dimension to the inquiry and makes it more enriched.

2. Materials and Methods

2.1. Sample collection and extract preparation

The experiment was carried out on *C. olitorius* and *M. oleifera* leaves and seeds samples. Samples of *C. olitorius* leaves and seeds were designated as COL and COS respectively while samples of *M. oleifera* leaves and seeds were designated as MOL and MOS respectively Aseptic samples were obtained from Bogura district, Bangladesh and were sent to the Microbiology Laboratory, Department of Genetic Engineering and Biotechnology, University of Rajshahi, Bangladesh. The disease-free samples were cleaned with 70% ethanol and then broken into powder by an electric grinding machine and placed in an incubator at 65 °C for appropriate drying. The methanolic extracts were prepared by mixing 25g powdered materials into 100 mL of solvents as per Mariswamy et al. [25]. The mixture was shaken on shaker for seven days and then adequately filtered with Whatman no. 1 filter paper. The filtered samples were evaporated at room temperature.

2.2. Antioxidant activity test

The antioxidant activity was measured by following method described by Rahman et al. [26]. The initial concentrations of each solvent extract were increased to 50, 100, 150, 200, and 250 μg/mL, then methanol was added to produce the volume 1 mL. By adding 1.5 mL of DPPH solution and then vials were left in the dark for 32 minutes. After 32 minutes, OD was measured at 517 nm with a spectrophotometer made in Germany by Analytik Jena. The procedure outlined by Jahan et al. [27] was used to create the BHT standard curve. Using the approach outlined by Mahmud et al., the

percentage of scavenging was determined by displaying the equation in an Excel linear scatter graph to determine the half maximum inhibitory concentration (IC_{50}) value [28].

2.4. Cytotoxic activity test

Using brine prawn nauplii (*Artemia salina*), the cytotoxic activity of these extracts was assessed using the procedure outlined by Meyer et al. [29]. For this, 48 hours of artificially generated 1% NaCl saltwater were used to hatch *Artemia salina*. Each extract's concentrations were changed to 25, 50, 100, 150, and 200 μg/mL. After that, 15 live brine prawns were placed in each vial with 5 milliliters of artificial saltwater and allowed to sit at room temperature for a whole day. The overall number of fatalities and survivors was tallied after a day.

2.6. In silico analysis

2.6.1. Ligand collection and preparation

We gathered *C. olitorius* and M. oleifera leaf and seed substances from relevant research findings and publications. These substances were ready to be used in the molecular docking investigation as ligands. The ligand structures were optimized and minimized using the mmff94 force field [30] and the steepest gradient technique.

2.6.2. Protein preparation

The RCSB PDB (Research Collaboratory for Structural Bioinformatics Protein Data Bank) provided the crystal structures of the human alpha-amylase (PDB ID: 3baj) and alpha-glucosidase (PDB ID: 3w37) domains [31]. The retrieved protein structure has been cleaned and processed by eliminating water molecules and heteroatoms using the most recent versions of PyMOL [32] and Discovery Studio [33]. The Swiss-PDB viewer [34] tool was used to optimize and minimize energy after crystal structure purification.

2.6.3. Molecular docking study

Molecular docking was performed with the PyRx virtual screening tool [35] to determine all possible conformations, orientations, and binding affinities of the ligands with the alpha-amylase and alpha-glucosidase proteins. All ligand free energy values were optimized with universal force field (UFF), conjugated gradient techniques and 2000 minimization steps. All ligands were converted to PDBQT format for docking with AutoDock Vina. This docking approach was designed to allow any ligand to spin with the protein fixed in place. The center and grid box sizes for each docked complex are shown in **Table 1**. The docking of protein-ligand complexes and analysis of docking poses were carried out using BIOVIA Discovery Studio. PyMOL and BIOVIA Discovery Studio were used for the exploration of non-bonding interactions. Docking studies were carried out to select the top two conformations for each protein based on their docking scores (in kcal/mol).

2.6.4. Molecular dynamics (MD) simulation study

The molecular dynamics (MD) simulation was conducted using the AMBER14 force field [36][37] and the YASARA software [38]. The docked complexes originally optimized, integrating additional hydrogen bond interactions. The TIP3P solvation model was exploited to determine the cubic simulation was conducted under constant boundaries [39][40][41]. In parallel, the establishment of a simulation cell regarding the protein and ligand enabled in a 20Å expansion of the counterfeit cell towards both pathways. The simulation cell's optimum physiological specifications are pH 7.4, 298 K, and 0.9% NaCl. Over around 5000 cycles of the steepest gradient technique, a significant energy mitigate was obtained by using the simulated annealing method. For the simulation cell, a constant time step of 1.25 fs was employed in the interim. Over around 5000 cycles of the steepest gradient technique, a significant energy mitigate was obtained by using the simulated annealing method. In the meantime, the simulation cell was programmed to a constant duration step of 1.25 fs. To estimate prolonged electrostatic interactions, the Particle Mesh Ewald approach was adopted with a cut-off radius of 8.0 Å [42][43][44][45]. The simulated paths were spaced apart every 100 ps. The simulation ran for 100 ns with constant temperature, pressure, and a Berendsen thermostat. Finally, the trajectory data was utilized to compute RMSD (root mean square deviation), Rg (radius of gyration), hydrogen bond, SASA (solvent accessible surface area), and RMSF (root mean square fluctuation) [46][47][48].

2.6.5. ADMET prediction

The pharmacokinetic parameters were determined using the ADMET (absorption, distribution, metabolism, excretion, and toxicity) predictions from reputable web servers such as SwissADME [49], pKCSM [50], and admetSAR [51].

2.7. Statistical analysis

For every biological sample, three replications of the study were conducted [52]. To find the significance mean±SD of each data group, Microsoft Excel version 2021 was used to calculate the mean and standard deviation. Graphical representations were created using Graph Pad Prism 8.

3. Results

3.1. DPPH scavenging activity

The DPPH scavenging percentage of both *C. olitorius* and *M. oleifera* extracts increased in proportion to the increasing concentration (**Figure 1a**). The IC_{50} values are the concentration necessary to scavenge 50% of free radicals. The IC_{50} values of *C. olitorius* leaves and seeds were 108.96 µg/mL and 139.67 µg/mL respectively while the IC_{50} values of *M. oleifera* leaves and seeds were 132.15 µg/mL and 174.86 µg/mL respectively (Figure 1.b) While the typical antioxidant BHT has an IC_{50} value of 152.21 µg/mL. Our results showed that the IC_{50} value of *C. olitorius* and *M. oleifera* extracts, especially the leaf extracts of M. oleifera, were lower than BHT. This result shows that *M. oleifera* leaves showed better antioxidant activity than other extracts as they reached 50% scavenging at 108.96 µg/mL higher than other extracts **(Figure 1b)**.

3.2. Cytotoxicity test

The cytotoxicity of these methanolic extract from *C. olitorius* and *M. oleifera* leaves and seeds are shown in **Figure 1c and d**. The LC_{50} values, indicating the concentration required to induce 50% mortality, were 202.60 and 146.71 µg/mL for *C. olitorius* leaves and seeds, respectively. For *M. oleifera*, the LC_{50} values were 160.25 µg/mL for the leaves and 120.83 µg/mL for the seeds. These results indicate that *C. olitorius* leaves exhibit lower cytotoxicity compared to the other extracts **(Figure 1d),** as they required a higher concentration of 202.60 µg/mL to achieve 50% mortality, suggesting they are less toxic than the other extracts tested.

3.3. Docking analysis

In this study, molecular docking research was undertaken for binding interactions of several phytochemicals with human alpha-amylase and alpha-glucosidase to discover the lead compounds for type 2 diabetes therapy. The docking results revealed that the binding energies of prunol and stigmasterol with human alpha amylase were -9.3 and -9.1 Kcal / mol, respectively (**Table 2**). The values were greater than that of control inhibitor acarbose with a docking score of −7.9 Kcal/mol. Additionally, rutin and apigetrin exhibited binding energies of -8.9 and -8.1 Kcal/mol respectively (**Table 2**), which are greater than acarbose with docking score −7.0 Kcal/mol. Prunol, apigetrin and stigmasterol were detected in *C. olitorius* extracts and rutin in *M. oliefera* extracts. Prunol demonstrated strong binding interactions with strong binding interactions with alpha-amylase, forming four conventional hydrogen bonds with the active site residues ARG252, PRO332, THR6, and GLY334, and a carbon-hydrogen bond with GLN8. Bonding distances measured at 2.21 Å, 2.58 Å, 2.26 Å, 3.03 Å, and 2.63 Å, respectively (**Figure 2c and Table 2**). Additionally, an alkyl interaction with PRO4 was observed at 4.29 Å (**Figure 2c and Table 2**).

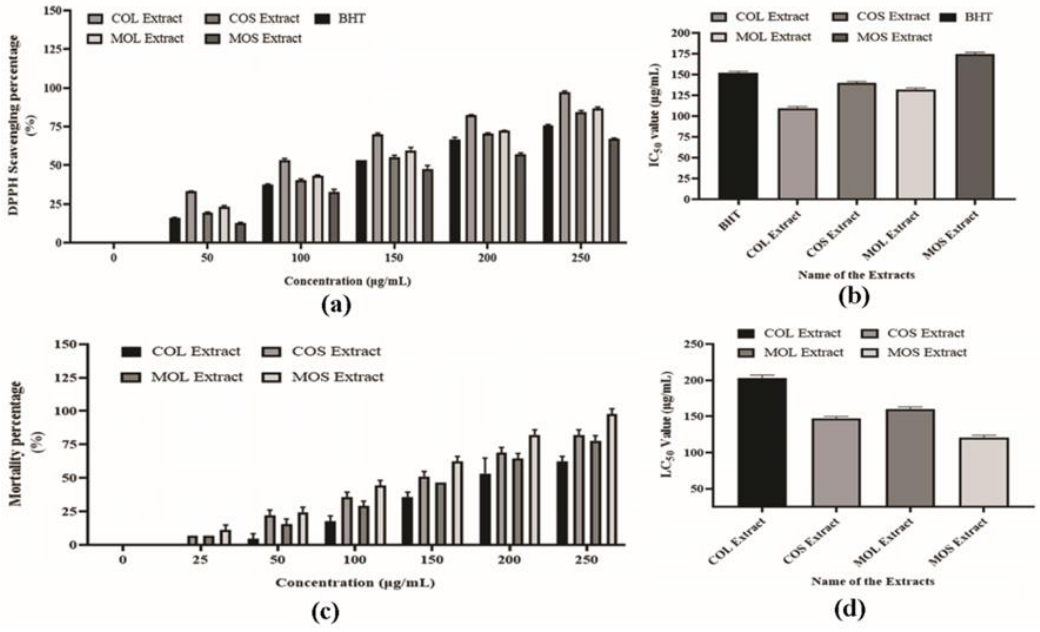

Figure 1. Antioxidant and cytotoxic activity of *C. olitorius* and *M. oleifera* plant leaves and seeds extract. Here, **(a)** indicates scavenging percentage of these extracts, **(b)** indicates IC_{50} values, **(c)** indicates the mortality percentages of these extracts, and (**d)** indicates LC_{50} values. These columns indicate significant differences between mean ± SD.

Stigmasterol also formed significant interactions with alpha-glucosidase, including a conventional hydrogen bond with GLU235 and alkyl bonds with LEU162, LEU165, and ALA198, as well as a pi-alkyl bond TRP59 at distances of 4.64 Å (**Figure 2f and Table 2**). In comparison, the control molecule acarbose formed five conventional hydrogen bonds with the alpha-glucosidase active site residues ARG252, ARG421, THR6, ARG10, and ASP402, along with carbon hydrogen bonds at THR6 and alkyl interaction at PRO4 a pi-alkyl bond was observed with PHE335 (**Figure 2i and Table 2**). Rutin showed strong interactions with alpha-glucosidase, forming five conventional hydrogen bonds with residues ASP568, SER474, HIS626, ASP469, and TRP432.Additional interactions included pi-alkyl interactions at TRP467, TRP565, PHE601, LYS506, and HIS626, a pi-anion bond with ASP232, a pi- pi stacked bond at PHE476, and a pi-donor hydrogen bond at TRP329 residues (**Figure 3.c and Table 2**). Apigetrin stabilized by six conventional hydrogen bonds at GLU105, ARG102, ARG103, GLU109, PRO114, and ARG93, also formed alkyl bonds with PRO107 (**Figure 3f and Table 2**). Moreover, the control acarbose formed four conventional hydrogen bonds with ASN572, ILE698, ASP697, and ASN572, along with carbon hydrogen bonds at PRO238 (**Figure 3i and Table 2**).

Table 1. The box size and box of docked pose in AutoDock Vina.

Protein	Center (Å)	Dimension (Å)
Alpha-amylase	X=8.3262, Y=28.6295, Z=50.178	X=58.6537, Y=56.5786, Z=46.1378
Alpha-glucosidase	X=16.5014, Y=8.3050, Z=123.9474	X=49.4324, Y=75.0238, Z=59.1801

3.5. Molecular dynamics simulation

Molecular dynamics simulation was employed to validate the docking conditions for the top three complexes involving proteins such as, alpha-amylase-prunol, alpha-amylase-stigmasterol, alpha-amylase-acarbose, alpha-glucosidase-apigetrin, alpha-glucosidase-acarbose, and alpha-glucosidase-rutin, as well as the rigidity of these structures. The RMSD value for the C-alpha atoms was determined to evaluate the differences in the stability of the complex produced by the ligand and protein based on the simulation processes' trajectories. In the **Figure 5a** showed the RMSD profiles of three distinct molecular complexes over a 100 ns simulation time.

Table 2. Non-bond interactions of the ligand molecules with the three target proteins of alpha-amylase and the alpha-glucosidase.

Complex	Binding Affinity (Kcal/mol)	Residues contact	Bond type	Distance in Å
Alpha-amylase-prunol (64945)	-9.3	ARG252	H	2.20831
		GLY334	H	3.03534
		PRO332	H	2.57556
		THR6	H	2.25567
		GLN8	Carbon H	2.62956
		PRO4	Alkyl	4.28785
		PRO4	Alkyl	4.88803
Alpha-amylase-acarbose (41774)	-7.9	ARG252	H	2.37823
		ARG421	H	2.08248
		THR6	H	2.76532
		ARG10	H	2.03368
		ASP402	H	1.9821
		THR6	Carbon H	2.92514
		PRO4	Alkyl	4.51243
		PHE335	Pi-Alkyl	4.65795
Alpha-amylase-stigmasterol (5280794)	-9.1	GLU235	H	2.33497
		TRP59	Pi-Alkyl	4.64896
		LEU162	Alkyl	5.15627
		LEU165	Alkyl	4.72471
		ALA198	Alkyl	4.84502
Alpha-glucosidase-rutin (5280805)	-8.9	ASP568	H	2.53016
		SER474	H	1.79019
		HIS626	H	2.44956
		ASP469	H	1.94374

		TRP432	H	2.38486
		TRP467	Pi-Alkyl	5.19208
		TRP565	Pi-Alkyl	4.88629
		PHE601	Pi-Alkyl	4.79297
		LYS506	Pi-Alkyl	4.08588
		HIS626	Pi-Alkyl	5.26934
		ASP232	Pi-Anion	3.9305
		PHE476	Pi- Pi Stacked	3.77936
		TRP329	Pi-Donor H	3.03303
Alpha-glucosidase-apigetrin (5280704)	-8.1	GLU105	H	2.42633
		ARG102	H	2.53044
		ARG103	H	2.65462
		GLU109	H	2.28309
		PRO114	H	2.75481
		ARG93	H	2.12672
		PRO107	Pi-Alkyl	4.42456
Alpha-glucosidase-acarbose (41774)	-7.0	ASN572	H	2.40677
		ILE698	H	2.53468
		ASP697	H	2.07545
		ASN572	H	2.93659
		PRO238	H	3.3942

In comparison to the other two complexes, alpha-amylase-acarbose showed a gradual, steady increase in RMSD value, eventually reaching the highest average values toward the end of the timeline. The alpha-amylase-prunol complex showed an early, rapid increase in RMSD within the initial 10 ns and fluctuated with relatively high amplitude between 15 to 40 ns but achieves a more stable and constant RMSD value from 40 to 65 ns. Furthermore, the alpha-amylase-stigmasterol complex displayed a highly stable RMSD value from 40 to 70 ns of simulation time, remaining mostly stable for the rest of the simulation time with minor fluctuations. For most of the simulation, the RMSD value for the alpha-amylase-acarbose complex hovers close to 1.25Å, whereas the RMSD value for the alpha-amylase-stigmasterol complex stayed lower, generally below 1.15Å for most of the run. The alpha-amylase-prunol complex's higher early fluctuation suggested initial structural instability across the early stages of simulation compared to the others. Therefore, compared to the Acarbose and Prunol complexes, the alpha-amylase-stigmasterol complex is expected to be structurally more stable. Similarly, **Figure 5a** displayed the RMSD of the 3W37 protein complexes with three different ligands over a 100 ns molecular dynamics simulation. In comparison to the other two complexes, the alpha-glucosidase-acarbose complex exhibited the highest average increase in RMSD value, peaking near 1.4Å around the 55 ns. The alpha-glucosidase-apigetrin complex showed an initial sharp spike up to 1.3Å within the first 10 ns but established a relatively constant and lower RMSD value (averaging around 1.15Å) from 20 to 60 ns. Meanwhile, the alpha-glucosidase-rutin complex exhibited a steady, gradual increase before stabilizing after 70 ns of simulation time, remaining stable for the rest of the period with minor fluctuations around 1.25Å. For most of the simulation, all three complexes remained highly stable as their RMSD values stay well below 1.5Å. However, the slightly lower and more consistent RMSD profile of the alpha-glucosidase-apigetrin complex suggested it may possess greater structural stability and rigidity during the simulation compared to the Acarbose and Rutin complexes.

The SASA value of the complexes was measured as well to better comprehend how the surface region of the alpha-amylase, and 3W37 proteins evolved gradually after contact with their respective top three ligands. The protein's surface area is increasing when the SASA number rises, and it is contracting when the value falls [14]. In **Figure 4b**, the alpha-amylase-acarbose, alpha-amylase-prunol, and alpha-amylase-stigmasterol complexes showed the increasing SASA value entire the simulation time. Among them, the alpha-amylase-acarbose, and alpha-amylase-prunol exhibited a larger SASA than the alpha-amylase-stigmasterol complex, implying that alpha-amylase-acarbose, and alpha-amylase-prunol had a more widespread surface compared to alpha-amylase-stigmasterol. In terms of the 3W37 protein, the 3W37-acarbose complex had an expanded surface than the other complexes, as illustrated by its significantly higher SASA at a simulation period of 0-25 ns, and 35–100 ns (**Figure 5.b**). The alpha-glucosidase-rutin and alpha-glucosidase-apigetrin complexes

attained a steady state at 15 ns and 40 ns simulation durations, respectively, and remained firm for the remainder of the simulation time with mild turbulence.

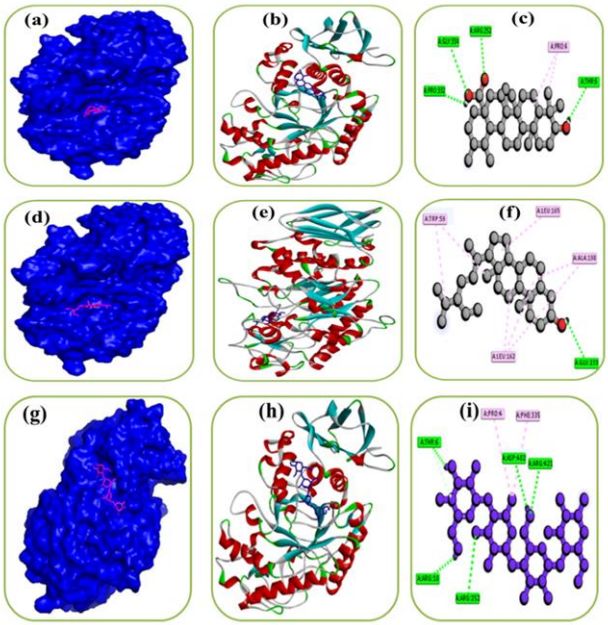

Figure 2. Molecular interactions of the selected compound with alpha-amylase, **(a)- (c)** prunol with alpha-amylase, **(d)-(f)** stigmasterol with alpha-glucosidase, **(g)-(i)** control acarbose with alpha-glucosidase.

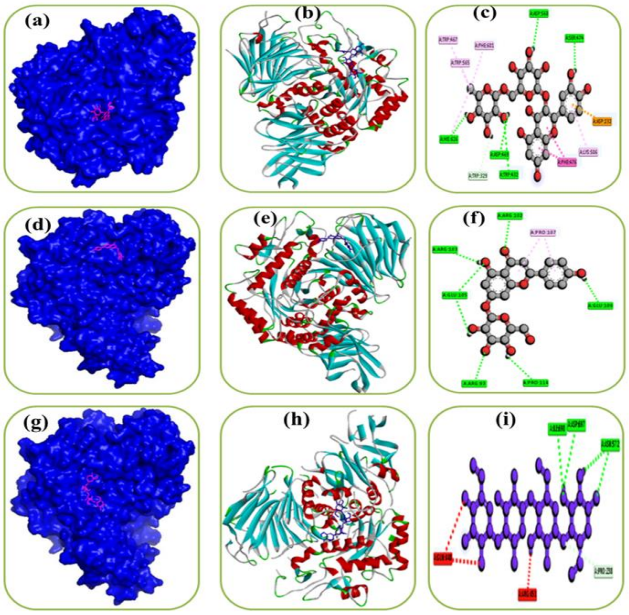

Figure 3. Molecular interactions of the selected compound with alpha-glucosidase, **(a)- (c)** rutin with alpha-glucosidase, **(d)-(f)** apigetrin with alpha-glucosidase, **(g)-(i)** control acarbose with alpha-glucosidase.

Rg values were used to determine the degree of compactness or flexibility of the protein complexes. In a simulated protein complex, a greater Rg value denotes flexibility, whereas a lower number denotes rigidity [15]. In **Figure 4c**, the alpha-amylase-acarbose complex had an average Rg value that was greater than the other complexes with alterations. The alpha-amylase-acarbose complex displayed the highest Rg value during the 30-50 ns time frame, whereas the alpha-amylase-prunol complex displayed the highest Rg value across the 0–10 ns and 65–100 ns time frames, and meanwhile alpha-amylase-stigmasterol displayed the lowest Rg value comped to the other two complexes throughout the time. Like this, in Figure **5.c** the alpha-glucosidase-acarbose, and alpha-glucosidase-epigetrin complexes showed the greatest Rg value during the almost 100 ns simulated period, whereas the alpha-glucosidase-Rutin complex showed the lowest Rg value overall with just minor variations. These findings conclude that compared to the alpha-glucosidase-acarbose, and alpha-glucosidase-epigetrin complexes, the alpha-glucosidase-rutin complex is relatively less flexible. Due to the hydrogen bonds importance to protein stability and integrity, the hydrogen bond-forming ability of the resulting docking complexes was analyzed. A large network of hydrogen bonds was formed in the alpha-amylase-acarbose, alpha-amylase-prunol, and alpha-amylase-stigmasterol complex during the period of the simulation, emphasizing that the three top three ligand molecules assembled a robust integration with the alpha-amylase protein (**Figure 4d**). Similarly, the alpha-glucosidase-acarbose, alpha-glucosidase-apigetrin, and alpha-glucosidase-rutin complexes built an enormous network of hydrogen bonds throughout the period of the simulation, emphasizing that the top three ligand molecules created a strong interaction with the 3W37 protein (**Figure 5d)**.

The RMSF values of the six protein-ligand complexes have been assessed to gain an understanding of the protein's ability to bind across amino acid residues. With only a few minor outliers, the RMSF profiles of the alpha-amylase-acarbose, alpha-amylase-prunol, alpha-amylase-stigmasterol, alpha-glucosidase-acarbose, alpha-glucosidase-apigetrin, and alpha-glucosidase-rutin complexes were below 2.5 Å (**Figure 4e**; **Figure 5e)**. The top three docked complexes for the protein exhibit less flexibility due to lower RMSF values, which is consistent with its better stability, as lower RMSF values reflect a more stable complex [14].

3.5.3. ADMET prediction

The effectiveness and safety of the top two candidate compounds for each protein were assessed using a variety of ligand characteristics, such as pharmacokinetics and toxicity profiles (**Table 3**). There were 2, 1, 16, and 10 hydrogen bond acceptors and 2, 1, 10, and 6 hydrogen bond donors in the substances prunol, stigmasterol, rutin, and apigetrin, respectively. For prunol, stigmasterol, rutin, and apigetrin, the topological polar surface area (TPSA) was 201.354 Å², 186.349 Å², and

174.313 Å², respectively. Pharmacokinetically, drugs with high gastrointestinal (GI) absorption included riboprine, Z-Gly-Pro, and 4-hydroxyretinoic acid, whereas compounds with low GI absorption included succinyladenosine, xanthosine, and 2'-deoxyinosine-5'-monophosphate. All the top compounds were shown to be impermeable to the blood-brain barrier (BBB), except for 4-hydroxyretinoic acid. Additionally, toxicity profiling revealed no evidence of skin sensitisation for any of the tested chemicals. Furthermore, every compound aside from succinyl adenosine—complied with Lipinski's Rule of Five.

4. Discussion

C. olitorius leaves exhibit lower cytotoxicity compared to the other extracts (**Figure 1d**), as they required a higher concentration of 202.60 µg/mL to achieve 50% mortality, suggesting they are less toxic than the other extracts tested. Several research studies have been demonstrated that compounds from *C. olitorius* and *M. oleifera* can serve as alternative sources for the treatment of human disease[53], [54], [55], [56]. This study focused on examining the antioxidant and cytotoxicity activity of *C. olitorius* and *M. oleifera* leaf and seed extract which examining the inhibitor effects of alpha-amylase and alpha-glucosides by assessing the binding affinities of these plants' phytochemicals through *in silico* molecular docking and molecular simulations. Both *C. olitorius* and *M. oleifera* leaf and seed extract exhibit notable antioxidant activity, with scavenging percentage increase with concentrations. The IC_{50} values for the leaf extract of *C. olitorius* (108.96 µg/mL) and *M. oleifera* (132.15 µg/mL) were lower than the synthetic antioxidant BHT (152.21µg/mL), indicating stronger antioxidant potential in these extracts.

Table 3. Pharmaceutical profiles generated from the SwissADME, admetSAR and pKCSM webservers for the top two probable candidates for each protein from docking.

Parameters	Prunol	Stigmasterol	Rutin	Apigetrin	Acarbose
Molecular weight (g/mol)	456.7	412.7 g/mol	610.5 g/mol	432.4 g/mol	472.7 g/mol
Num. of H-bond acceptors	2	1	16	10	3
Num. of H-bond donors	2	1	10	6	3
SASA (Å²)	201.354	186.349	240.901	174.313	206.148
Caco-2 permeability	0.8353	0.7953	0.9172	0.9208	0.7175
AMES toxicity	No	No	No	Yes	No
P-glycoprotein inhibitor	No	No	No	No	No
Carcinogenicity	No	No	No	No	No
BBB permeability	No	Yes	No	No	Yes
Skin sensitization	No	No	No	No	No
Lipinski rule of five	Yes; 0 violation	Yes; 0 violation	No; 0 violations	Yes; 0 violation	Yes; 0 Violation

Among the extracts, *M. oleifera* leaves demonstrated the most potential antioxidant activity, achieving 50% free radical scavenging at a lower concentration compared to other samples. This is consistent with previous research highlighting *M. oleifera* as a rich source of bioactive compounds with antioxidant capacity [57], [58]. These findings suggest the potential for utilizing *M. oleifera* and *C. olitorius* as natural alternatives synthetic antioxidants in health applications. The cytotoxicity assessment of methanolic extracts from *C. olitorius* and *M. oleifera* leaves and seeds revealed varying degrees of toxicity, with the LC_{50} values indicating the concentration required for 50% mortality. *C. olitorius* leaves exhibited the highest LC_{50} values of 202.60 µg/mL, suggesting lower cytotoxicity compared to the seed extracts of species, as well as *M. oleifera* leaves and seeds. These findings align with previous studies that have shown differing levels of toxicity in plant extracts, emphasizing the influence of plant part and extract concentration on biological activity [59], [59], [60]. The lower toxicity observed in *C. olitorius* leaves suggests that they may hold potential for safer use in therapeutic applications, aligning with findings by other researchers who have noted the medicinal benefits of *C. olitorius* species with minimal adverse effects [53], [61], [62]. Further investigation is necessary to identify the specific bioactive compounds responsible for these effects and to evaluate their potential therapeutic use in safe dosages [63], [64], [65].

The molecular docking analysis conducted on various phytochemicals from *C. olitorius* and *M. oleifera* revealed promising binding interactions with human alpha-amylase and alpha-glucosidase, highlighting their potential as lead compounds for type 2 diabetes treatment. Prunol and stigmasterol exhibited strong binding affinities for alpha-amylase, with docking scores of -9.3 and -9.1 Kcal/mol, respectively outperforming the control inhibitor acarbose, which had docking scores of -7.9 Kcal/mol. Prunol demonstrated particularly strong interactions, forming multiple hydrogen bonds with the enzymes active site residues (ARG252, PRO332, and GLY334), along with additional alkyl interactions, suggesting its potential as a potent alpha-amylase inhibitor. For alpha-glucosides, rutin and apigetrin displayed stronger binding than

acarbose, with binding energies of -8.9 and -8.1 Kcal/mol, respectively, underscoring their higher affinity for the enzyme. Rutin formed several hydrogen bonds and pi interactions, indicating its stability within the enzymes active site, while apigetrin also showed significant binding with key resides, further enhancing its potential as an effective inhibitor. The interactions observed for these phytochemicals align with previous studies showing that plant-derived compounds can effectively modulate enzyme activity, offering novel therapeutic approaches for managing type 2 diabetes [66], [67], [68], [69]. The findings suggest that the phytochemicals in *C. olitorius* and *M. oleifera* may offer promising natural alternatives or adjuvants to current pharmaceutical treatments for diabetes [70], [71], [72].

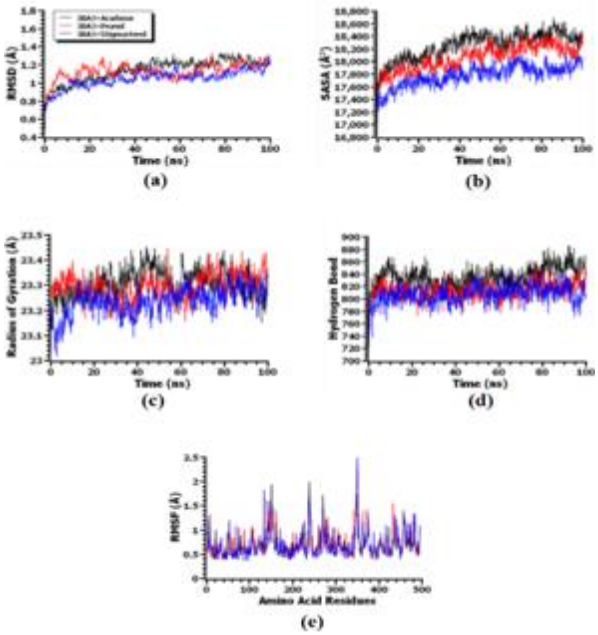

Figure 4. The alphabetic order **(a)-(e)** shows the following- **(a)** RMSD, **(b)** SASA, **(c)** Rg, **(d)** number of hydrogen bonds and **(e)** RMSF calculated from molecular dynamics simulation of alpha-amylase-acarbose, alpha-amylase-prunol and alpha-amylase-stigmasterol complexes at 298K temperature.

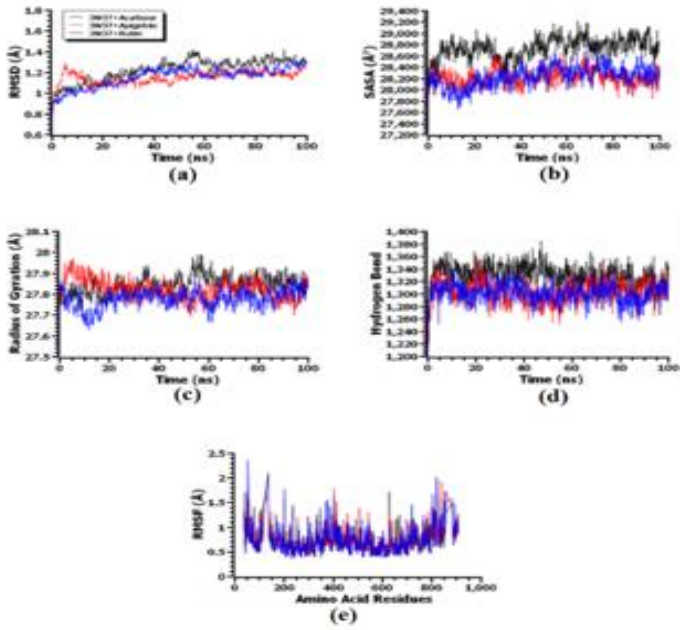

Figure 5. The alphabetic order **(a)-(e)** shows the following: **(a)** RMSD, **(b)** SASA, **(c)** Rg, **(d)** number of hydrogen bonds and **(e)** RMSF, calculated from the molecular dynamics simulation of of alpha-glucosidase-acarbose, alpha-glucosidase-apigetrin and alpha-glucosidase-rutin at 298K temperature.

The molecular dynamics of simulations conducted to assess the stability of the docked complexes with alpha-amylase and alpha-glucosidase revealed critical insights into the nature of the binding interactions. The analysis of root mean square deviations (RMSD) showed that both the alpha-amylase and alpha-glucosidase complexes reached a stedy state after initial fluctuations, indicating the stable binding of the ligands within the active sites. The RMSD values remained consistently below 2.5 Å, suggesting that the docked complexes maintained their structural integrity throughout the simulation. Additionally, the solvent accessible surface area (SASA) analysis demonstrated that both alpha-amylase and alpha-glucosidase complexes exhibited stable SASA trends, with no significant fluctuations, indicating the rigidity of the complexes in their bound states. The radius of gyration (Rg) analysis further supported these findings, showing that the alpha-glucosidase complexes exhibited a more stable Rg profile, while the alpha-amylase complexes displayed slightly higher Rg values, reflecting a more flexible nature during interactions. Hydrogen bond analysis also corroborated the stable nature of the complexes, as the number of hydrogen bonds remained relatively constant throughout the simulations. These results highlight the potential of the identified phytochemicals as stable and effective inhibitors of both enzymes, suggesting their promise in therapeutic applications for type 2 diabetes management [66], [73], [74], [75].

5. Conclusion

This study provides compelling evidence for the potential of *C. olitorius* and *M. oleifera* leaves and seeds as promising sources of bioactive compounds for the management of type 2 diabetes. The *in-silico* analyses revealed significant inhibitory effects of phytochemicals from both alpha-amylase and alpha-glucosides enzymes, which play crucial role in carbohydrate metabolism. The antioxidant and cytotoxicity assays further highlighted the therapeutic potential of these plants, with both showing substantial antioxidant activity and relatively low toxicity, especially in leaf extracts. The molecular docking

studies identified key bioactive compounds such as prunol, stigmasterol, rutin, and apigetrin, with strong binding affinities to target enzymes, suggesting their potential as effective inhibitors. Additionally, molecular dynamic simulations demonstrated their stability and strong interaction with the enzymes, reinforcing their promise as competitive inhibitors. The favorable ADMET profiles also suggest that these compounds could be viable candidates for drug development, with suitable pharmacokinetics, and safety properties. Despite these promising results, further validation through *in vitro*, *in vivo*, and chemical studies is necessary to confirm the efficacy of these compounds in managing type 2 diabetes. This research paves the way for further exploration of these plants and bioactive constituents as potential therapeutic agents for diabetes management.

Author Contributions: G.K.P conceptualized, designed, and finalized the experiment. G.K.P performed all the experiments, analyzed data, and prepared the manuscript. M.A.S helped write the manuscript. M.A.S supervised the data analysis and revised the manuscript. All authors have read and agreed to the published version of the manuscript.

Funding: This research has not taken any funds.

Data Availability: The data presented in the study are included in the article/supplementary material.

Conflicts of Interest: The authors declare no conflict of interest.

References

[1] E. C. Estevam *et al.*, "Inspired by nature: The use of plant-derived substrate/enzyme combinations to generate antimicrobial activity in situ," *Nat. Prod. Commun.*, vol. 10, no. 10, pp. 1733–1738, 2015, doi: 10.1177/1934578x1501001025.

[2] Y. A. Attia and M. A. Al-Harthi, "Schwarzkümmelsamenöl als Alternative zu antibiotischen Leistungsförderern bei Masthühnern," *Eur. Poult. Sci.*, vol. 79, no. March, pp. 1–12, 2015, doi: 10.1399/eps.2015.84.

[3] M. E. Abd El-Hack *et al.*, "Cinnamon (Cinnamomum zeylanicum) oil as a potential alternative to antibiotics in poultry," *Antibiotics*, vol. 9, no. 5, pp. 1–12, 2020, doi: 10.3390/antibiotics9050210.

[4] S. Ben-Shabat, L. Yarmolinsky, D. Porat, and A. Dahan, "Antiviral effect of phytochemicals from medicinal plants: Applications and drug delivery strategies," *Drug Deliv. Transl. Res.*, vol. 10, no. 2, pp. 354–367, 2020, doi: 10.1007/s13346-019-00691-6.

[5] Y. A. Attia *et al.*, "Phytogenic Products and Phytochemicals as a Candidate Strategy to Improve Tolerance to Coronavirus," *Front. Vet. Sci.*, vol. 7, 2020, doi: 10.3389/fvets.2020.573159.

[6] N. Calland, J. Dubuisson, Y. Rouillé, and K. Séron, "Hepatitis C virus and natural compounds: A new antiviral approach?," *Viruses*, vol. 4, no. 10, pp. 2197–2217, 2012, doi: 10.3390/v4102197.

[7] Q. F. Hu *et al.*, "Antiviral phenolic compounds from Arundina gramnifolia," *J. Nat. Prod.*, vol. 76, no. 2, pp. 292–296, 2013, doi: 10.1021/np300727f.

[8] P. Samuelson, "Economic Calculation in the Socialist Commonwealth by Ludwig von Mises (1920)," *Econ. Theory*, no. 1920, pp. 1–32, 1990.

[9] R. Rahmad *et al.*, "Antibacterial cream formulation of ethanolic Pliek U extracts and ethanolic residue hexane Pliek U extracts against Staphylococcus aureus," *IOP Conf. Ser. Mater. Sci. Eng.*, vol. 523, no. 1, 2019, doi: 10.1088/1757-899X/523/1/012011.

[10] E. Moghaddam *et al.*, "Baicalin, a metabolite of baicalein with antiviral activity against dengue virus," *Sci. Rep.*, vol. 4, pp. 1–8, 2014, doi: 10.1038/srep05452.

[11] R. Bai *et al.*, "SJP-L-5, a novel small-molecule compound, inhibits HIV-1 infection by blocking viral DNA nuclear entry Microbe-host interactions and microbial pathogenicity," *BMC Microbiol.*, vol. 15, no. 1, pp. 1–13, 2015, doi: 10.1186/s12866-015-0605-3.

[12] R. Kapoor, B. Sharma, and S. S. Kanwar, "Antiviral Phytochemicals: An Overview," *Biochem. Physiol. Open Access*, vol. 06, no. 02, 2017, doi: 10.4172/2168-9652.1000220.

[13] P. Cos, L. Maes, D. Vanden Berghe, N. Hermans, L. Pieters, and A. Vlietinck, "Plant Substances as Anti-HIV Agents Selected According to Their Putative Mechanism of Action," *J. Nat. Prod.*, vol. 67, no. 2, pp. 284–293, 2004, doi: 10.1021/np034016p.

[14] K. Hostettmann and A. Marston, "Twenty years of research into medicinal plants: Results and perspectives," *Phytochem. Rev.*, vol. 1, no. 3, pp. 275–285, 2002, doi: 10.1023/A:1026046026057.

[15] G. M. Cragg and D. J. Newman, "Biodiversity: A continuing source of novel drug leads," *Pure Appl. Chem.*, vol. 77, no. 1, pp. 7–24, 2005, doi: 10.1351/pac200577010007.

[16] N. R. Farnsworth, O. Akerele, A. S. Bingel, D. D. Soejarto, and Z. Guo, "Medicinal plants in therapy," *Bull. World Health Organ.*, vol. 63, no. 6, pp. 965–981, 1985, doi: 10.1016/0378-8741(87)90016-x.

[17] P. A. G. . De Smet, "Drug Therapy: Herbal remedies," *N. Engl. J. Med.*, vol. 347, no. 25, pp. 2046–2056, 2002.
[18] N. Earlia *et al.*, "GC/MS Analysis of Fatty Acids on Pliek U Oil and Its Pharmacological Study by Molecular Docking to Filaggrin as a Drug Candidate in Atopic Dermatitis Treatment," *Sci. World J.*, vol. 2019, 2019, doi: 10.1155/2019/8605743.
[19] N. Earlia, R. Rahmad, M. Amin, C. Prakoeswa, K. Khairan, and R. Idroes, "The potential effect of fatty acids from Pliek U on epidermal fatty acid binding protein: Chromatography and bioinformatic studies," *Sains Malaysiana*, vol. 48, no. 5, pp. 1019–1024, 2019, doi: 10.17576/jsm-2019-4805-10.
[20] S. Gayathri Devi, S. Sangeetha, and C. Mary Shoba Das, "Comparative evaluation of phytochemicals and antioxidant potential of Cleome viscose and Trichodesma indicum," *Int. J. Pharm. Sci. Rev. Res.*, vol. 23, no. 1, pp. 253–258, 2013.
[21] V. I. Lushchak, "Free radicals, reactive oxygen species, oxidative stress and its classification," 2014. doi: 10.1016/j.cbi.2014.10.016.
[22] I. Liguori *et al.*, "Oxidative stress, aging, and diseases," *Clin. Interv. Aging*, vol. 13, pp. 757–772, 2018, doi: 10.2147/CIA.S158513.
[23] T. AshokKumar, "Antioxidants: new-generation therapeutic base for treatment of polygenic disorders," *Curr. Sci.*, vol. 86, no. 8, pp. 1092–1102, 2004.
[24] M. Carocho and I. C. F. R. Ferreira, "A review on antioxidants, prooxidants and related controversy: Natural and synthetic compounds, screening and analysis methodologies and future perspectives," *Food Chem. Toxicol.*, vol. 51, no. 1, pp. 15–25, 2013, doi: 10.1016/j.fct.2012.09.021.
[25] "Chromatographic finger print analysis of steroids in Aerva lanata L by HPTLC technique.".
[26] M. M. Rahman, M. B. Islam, M. Biswas, and A. H. M. Khurshid Alam, "In vitro antioxidant and free radical scavenging activity of different parts of Tabebuia pallida growing in Bangladesh," *BMC Res. Notes*, 2015, doi: 10.1186/s13104-015-1618-6.
[27] I. Jahan *et al.*, "GC-MS phytochemical profiling, pharmacological properties, and in silico studies of chukrasia velutina leaves: A novel source for bioactive agents," *Molecules*, vol. 25, no. 15, 2020, doi: 10.3390/molecules25153536.
[28] S. Mahmud *et al.*, "Efficacy of phytochemicals derived from avicennia officinalis for the management of covid-19: A combined in silico and biochemical study," *Molecules*, vol. 26, no. 8, 2021, doi: 10.3390/molecules26082210.
[29] B. N. Meyer, N. R. Ferrigni, J. E. Putnam, L. B. Jacobsen, D. E. Nichols, and J. L. McLaughlin, "Brine shrimp: A convenient general bioassay for active plant constituents," *Planta Med.*, 1982, doi: 10.1055/s-2007-971236.
[30] T. A. Halgren, "Performance of MMFF94*," *Scope, Parameterization, J. Comput. Chem.*, vol. 17, pp. 490–519, 1996.
[31] P. W. Rose *et al.*, "The RCSB protein data bank: Integrative view of protein, gene and 3D structural information," *Nucleic Acids Res.*, vol. 45, no. D1, pp. D271–D281, 2017, doi: 10.1093/nar/gkw1000.
[32] W. L. DeLano, "The PyMOL Molecular Graphics System, Version 1.1," *Schr{ö}dinger LLC*, 2002, doi: 10.1038/hr.2014.17.
[33] D. Studio, "Dassault Systemes BIOVIA, Discovery Studio Modelling Environment, Release 4.5," *Accelrys Softw. Inc.*, 2015.
[34] L. T. Kaplan W, "Software review Swiss-PDB Viewer (Deep View)," *Brief. Bioinform.*, vol. 2, no. 2, pp. 195–197, 2001.
[35] S. Dallakyan and A. J. Olson, "Small-Molecule Library Screening by Docking with PyRx," J. E. Hempel, C. H. Williams, and C. C. Hong, Eds., New York, NY: Springer New York, 2015, pp. 243–250. doi: 10.1007/978-1-4939-2269-7_19.
[36] J. Wang, R. M. Wolf, J. W. Caldwell, P. A. Kollman, and D. A. Case, "Development and testing of a general Amber force field," *J. Comput. Chem.*, vol. 25, no. 9, pp. 1157–1174, 2004, doi: 10.1002/jcc.20035.
[37] S. Biswas *et al.*, "Prospective role of lupeol from Pterocarpus santalinus leaf against diabetes: An in vitro, in silico, and in vivo investigation," *Comput. Biol. Med.*, vol. 186, 2025, doi: 10.1016/j.compbiomed.2025.109680.
[38] H. Land and M. S. Humble, "Chapter 4 in Biocatalytic Investigations," vol. 1685, pp. 43–67, 2018, doi: 10.1007/978-1-4939-7366-8.
[39] M. F. Harrach and B. Drossel, "Structure and dynamics of TIP3P, TIP4P, and TIP5P water near smooth and atomistic walls of different hydroaffinity," vol. 174501, no. March 2005, 2015, doi: 10.1063/1.4872239.
[40] S. Biswas *et al.*, "An in silico approach to develop potential therapies against Middle East Respiratory Syndrome Coronavirus (MERS-CoV)," *Heliyon*, vol. 10, no. 4, 2024, doi: 10.1016/j.heliyon.2024.e25837.
[41] S. Islam *et al.*, "Multifaceted Analysis of Lactobacillus plantarum DMR14 Reveals Promising Antidiabetic Properties Through In Vivo Assays and Molecular Simulations," *J. Cell. Mol. Med.*, vol. 29, no. 2, 2025, doi: 10.1111/jcmm.70347.

[42] T. Darden, H. Lee, and L. G. Pedersen, "A smooth particle mesh Ewald method," vol. 8593, no. April 2021, pp. 8577–8593, 2022.
[43] E. Krieger, J. E. Nielsen, C. A. E. M. Spronk, and G. Vriend, "Fast empirical pKa prediction by Ewald summation," *J. Mol. Graph. Model.*, vol. 25, no. 4, pp. 481–486, 2006, doi: 10.1016/j.jmgm.2006.02.009.
[44] E. Krieger and G. Vriend, "New ways to boost molecular dynamics simulations.," *J. Comput. Chem.*, vol. 36, no. 13, pp. 996–1007, May 2015, doi: 10.1002/jcc.23899.
[45] S. Mahmud *et al.*, "Antiviral peptides against the main protease of SARS-CoV-2: A molecular docking and dynamics study," *Arab. J. Chem.*, vol. 14, no. 9, 2021, doi: 10.1016/j.arabjc.2021.103315.
[46] S. Biswas *et al.*, "Molecular Docking and Dynamics Studies to Explore Effective Inhibitory Peptides Against the Spike Receptor Binding Domain of SARS-CoV-2," *Front. Mol. Biosci.*, vol. 8, 2022, doi: 10.3389/fmolb.2021.791642.
[47] S. Islam *et al.*, "Biological Efficacy of Compounds from Stingless Honey and Sting Honey against Two Pathogenic Bacteria: An In Vitro and In Silico Study," *Molecules*, vol. 27, no. 19, 2022, doi: 10.3390/molecules27196536.
[48] M. R. Islam *et al.*, "Modified oxymatrine as novel therapeutic inhibitors against Monkeypox and Marburg virus through computational drug design approaches," *J. Cell. Mol. Med.*, vol. 28, no. 18, p. e70116, 2024, doi: 10.1111/jcmm.70116.
[49] A. Daina, O. Michielin, and V. Zoete, "SwissADME: A free web tool to evaluate pharmacokinetics, drug-likeness and medicinal chemistry friendliness of small molecules," *Sci. Rep.*, vol. 7, no. January, pp. 1–13, 2017, doi: 10.1038/srep42717.
[50] D. E. V. Pires, T. L. Blundell, and D. B. Ascher, "pkCSM: Predicting small-molecule pharmacokinetic and toxicity properties using graph-based signatures," *J. Med. Chem.*, vol. 58, no. 9, pp. 4066–4072, 2015, doi: 10.1021/acs.jmedchem.5b00104.
[51] H. Yang *et al.*, "AdmetSAR 2.0: Web-service for prediction and optimization of chemical ADMET properties," *Bioinformatics*, vol. 35, no. 6, pp. 1067–1069, 2019, doi: 10.1093/bioinformatics/bty707.
[52] G. K. Paul *et al.*, "Volatile compounds of Bacillus pseudomycoides induce growth and drought tolerance in wheat (Triticum aestivum L.)," *Sci. Rep.*, vol. 12, no. 1, 2022, doi: 10.1038/s41598-022-22354-2.
[53] A. Biswas *et al.*, "A Comprehensive Review of C. capsularis and C. olitorius: A Source of Nutrition, Essential Phytoconstituents and Pharmacological Activities," *Antioxidants*, vol. 11, no. 7, 2022, doi: 10.3390/antiox11071358.
[54] H. O. Adebo, L. E. Ahoton, F. J. B. Quenum, H. Adoukonou-Sagbadja, D. O. Bello, and C. A. A. M. Chrysostome, "Ethnobotanical Knowledge of Jute (Corchorus olitorius L.) in Benin," *European J. Med. Plants*, vol. 26, no. 1, pp. 1–11, 2018, doi: 10.9734/ejmp/2018/43897.
[55] A. R. Ben Yakoub, O. Abdehedi, M. Jridi, W. Elfalleh, M. Nasri, and A. Ferchichi, "Flavonoids, phenols, antioxidant, and antimicrobial activities in various extracts from Tossa jute leave (Corchorus olitorus L.)," *Ind. Crops Prod.*, vol. 118, pp. 206–213, 2018, doi: 10.1016/j.indcrop.2018.03.047.
[56] K. K. Sha'a, G. P. Clarkson, and S. P. Artimas, "Phytochemical analysis, proximate composition and antinutritional factors of Corchorus oliterius plant," *Int. J. Biol. Chem. Sci.*, vol. 13, no. 4, pp. 2147–2157, 2019, doi: 10.4314/ijbcs.v13i4.21.
[57] O. D. Oloruntola and S. O. Ayodele, "Phytochemical, Proximate and Mineral Composition, Antioxidant and Antidiabetic Properties Evaluation and Comparison of Mistletoe Leaves from Moringa and Kolanut Trees," *Turkish J. Agric. - Food Sci. Technol.*, vol. 10, no. 8, pp. 1524–1531, 2022, doi: 10.24925/turjaf.v10i8.1524-1531.5134.
[58] D. A. C. K. Dalukdeniya, K. L. S. R. De Silva, and R. M. U. S. K. Rathnayaka, "Antimicrobial Activity of Different Extracts of Leaves Bark and Roots of Moringa oleifera (Lam)," *Int. J. Curr. Microbiol. Appl. Sci.*, vol. 5, no. 7, pp. 687–691, 2016, doi: 10.20546/ijcmas.2016.507.078.
[59] A. Sharma, S. Joshi, and N. Kumar, "Antioxidant and antibacterial properties of," vol. 9, no. 4, pp. 9–10, 2015.
[60] K. Szlachetka, P. Kut, and A. Stępień, "Cytotoxic and anticancer activity of Moringa oleifera," *Eur. J. Clin. Exp. Med.*, vol. 18, no. 3, pp. 214–220, 2020, doi: 10.15584/ejcem.2020.3.9.
[61] M. M. Islam, "Biochemistry, Medicinal and Food values of Jute (Corchorus capsularis L. and C. olitorius L.) leaf: A Review," *Int. J. Enhanc. Res. Sci. Technol. Eng.*, vol. 2, no. 11, pp. 35–44, 2013, [Online]. Available: http://www.erpublications.com/uploaded_files/download/download_27_11_2013_06_45_32.pdf
[62] M. A. M. Abdel-Razek, M. F. Abdelwahab, U. R. Abdelmohsen, and A. N. E. Hamed, "Pharmacological and phytochemical biodiversity of Corchorus olitorius," *RSC Adv.*, vol. 12, no. 54, pp. 35103–35114, 2022, doi: 10.1039/d2ra07406k.

[63] A. Pareek *et al.*, "Moringa oleifera: An Updated Comprehensive Review of Its Pharmacological Activities, Ethnomedicinal, Phytopharmaceutical Formulation, Clinical, Phytochemical, and Toxicological Aspects," *Int. J. Mol. Sci.*, vol. 24, no. 3, 2023, doi: 10.3390/ijms24032098.

[64] B. Padayachee and H. Baijnath, "An updated comprehensive review of the medicinal, phytochemical and pharmacological properties of Moringa oleifera," *South African J. Bot.*, vol. 129, pp. 304–316, 2020, doi: 10.1016/j.sajb.2019.08.021.

[65] O. Awodele, I. A. Oreagba, S. Odoma, J. A. Teixeira Da Silva, and V. O. Osunkalu, "Toxicological evaluation of the aqueous leaf extract of Moringa oleifera Lam. (Moringaceae)," *J. Ethnopharmacol.*, vol. 139, no. 2, pp. 330–336, 2012, doi: 10.1016/j.jep.2011.10.008.

[66] J. Riyaphan, D. C. Pham, M. K. Leong, and C. F. Weng, "In silico approaches to identify polyphenol compounds as α-glucosidase and α-amylase inhibitors against type-ii diabetes," *Biomolecules*, vol. 11, no. 12, 2021, doi: 10.3390/biom11121877.

[67] H. Rasouli, S. M. B. Hosseini-Ghazvini, H. Adibi, and R. Khodarahmi, "Differential α-amylase/α-glucosidase inhibitory activities of plant-derived phenolic compounds: A virtual screening perspective for the treatment of obesity and diabetes," *Food Funct.*, vol. 8, no. 5, pp. 1942–1954, 2017, doi: 10.1039/c7fo00220c.

[68] C. G. Kato-Schwartz *et al.*, "Potential anti-diabetic properties of Merlot grape pomace extract: An in vitro, in silico and in vivo study of α-amylase and α-glucosidase inhibition," *Food Res. Int.*, vol. 137, 2020, doi: 10.1016/j.foodres.2020.109462.

[69] H. Kashtoh and K. H. Baek, "New Insights into the Latest Advancement in α-Amylase Inhibitors of Plant Origin with Anti-Diabetic Effects," *Plants*, vol. 12, no. 16, 2023, doi: 10.3390/plants12162944.

[70] O. Sakulkeo, C. Wattanapiromsakul, T. Pitakbut, and S. Dej-Adisai, "Alpha-Glucosidase Inhibition and Molecular Docking of Isolated Compounds from Traditional Thai Medicinal Plant, Neuropeltis racemosa Wall.," *Molecules*, vol. 27, no. 3, 2022, doi: 10.3390/molecules27030639.

[71] H. Xiang *et al.*, "Inhibition mechanism of α-glucosidase by three geranylated compounds: Kinetic, spectroscopic and molecular docking," *Process Biochem.*, vol. 136, pp. 237–244, 2024, doi: 10.1016/j.procbio.2023.11.034.

[72] S. Ghosh and L. Rangan, "Molecular Docking and Inhibition Kinetics of α-glucosidase Activity by Labdane Diterpenes Isolated from Tora Seeds (Alpinia nigra B.L. Burtt.)," *Appl. Biochem. Biotechnol.*, vol. 175, no. 3, pp. 1477–1489, 2015, doi: 10.1007/s12010-014-1366-4.

[73] F. Khan, M. V. Khan, A. kumar, and S. Akhtar, "Recent Advances in the Development of Alpha-Glucosidase and Alpha-Amylase Inhibitors in Type 2 Diabetes Management: Insights from In silico to In vitro Studies," *Curr. Drug Targets*, vol. 25, 2024, doi: 10.2174/0113894501313365240722100902.

[74] G. A. Mohamed, A. M. Omar, M. E. El-Araby, S. Mass, and S. R. M. Ibrahim, "Assessments of Alpha-Amylase Inhibitory Potential of Tagetes Flavonoids through In Vitro, Molecular Docking, and Molecular Dynamics Simulation Studies," *Int. J. Mol. Sci.*, vol. 24, no. 12, 2023, doi: 10.3390/ijms241210195.

[75] M. A. Kausar *et al.*, "Identifying the alpha-glucosidase inhibitory potential of dietary phytochemicals against diabetes mellitus type 2 via molecular interactions and dynamics simulation," *Cell. Mol. Biol.*, vol. 67, no. 5, pp. 16–26, 2021, doi: 10.14715/CMB/2021.67.5.3.